NJC

Accepted Manuscript

This is an *Accepted Manuscript*, which has been through the Royal Society of Chemistry peer review process and has been accepted for publication.

Accepted Manuscripts are published online shortly after acceptance, before technical editing, formatting and proof reading. Using this free service, authors can make their results available to the community, in citable form, before we publish the edited article. We will replace this *Accepted Manuscript* with the edited and formatted *Advance Article* as soon as it is available.

You can find more information about *Accepted Manuscripts* in the Information for Authors.

Please note that technical editing may introduce minor changes to the text and/or graphics, which may alter content. The journal's standard Terms & Conditions and the Ethical guidelines still apply. In no event shall the Royal Society of Chemistry be held responsible for any errors or omissions in this *Accepted Manuscript* or any consequences arising from the use of any information it contains.

ROYAL SOCIETY OF CHEMISTRY

www.rsc.org/njc

Table of content entry

Fabricating $BaZrO_3$ Hollow Microspheres by a Simple Reflux Method

Yongcun Zou*[a], Yang Luo[b], Ni Wen[b], Tiannan Ye[b], Caiyun Xu[b], Jianguo Yu[b], Fengqin Wang[b], Guodong Li[a], and Yongnan Zhao*[b]

$BaZrO_3$, $SrZrO_3$ and $SrHfO_3$ hollow microparticles were prepared by a reflux method. The greatly concentrated KOH solution initiated a grain nucleation to reduce the particle sizes and afforded a high reaction temperature to promote the hollowing process.

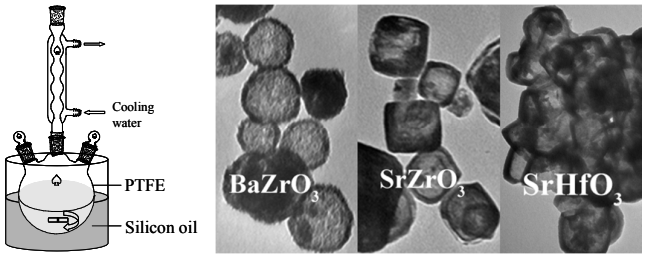

Cite this: DOI: 10.1039/c0xx00000x

www.rsc.org/xxxxxx

ARTICLE TYPE

Fabricating $BaZrO_3$ Hollow Microspheres by a Simple Reflux Method

Yongcun Zou*[a], Yang Luo[b], Ni Wen[b], Tiannan Ye[b], Caiyun Xu[b], Jianguo Yu[b], Fengqin Wang[b], Guodong Li[a], and Yongnan Zhao*[b]

Received (in XXX, XXX) Xth XXXXXXXXX 20XX, Accepted Xth XXXXXXXXX 20XX

DOI: 10.1039/b000000x

A simple reflux method was developed to fabricate hollow microparticles of complex oxide. Single crystalline perovskite-type $BaZrO_3$ hollow microspheres have been synthesized in a concentrated KOH solution via Ostwald ripening. The heavily increased KOH concentration directed to the increase of supersaturation of the reactants and a grain growth of primary particulates that readily agglomerated into the aggregated particles. The greatly elevated KOH concentration also decreased the aggregated particle sizes due to the enhanced interparticle attractive force. Heat treatment promoted the hollowing process. Refluxing a mixture in 20 mol L^{-1} KOH solutions in a 200 ℃ oil bath produced perovskite $BaZrO_3$ hollow microspheres with an average size of 92 nm. XRD patterns indicated the cubic perovskite structure of $BaZrO_3$ hollow microspheres. HRTEM and SAED measurements disclosed the single crystal nature of a single $BaZrO_3$ hollow microsphere. The products experienced morphology variations of solid, core-shell and hollow microspheres at various reaction durations. The greatly concentrated KOH solution not only led to a smaller aggregated particle sizes but also gave a high boiling temperature to accelerate the diffusion rate and promote the ripening process. Similarly, perovskite $SrZrO_3$ and $SrHfO_3$ hollow microparticles were also fabricated by this method.

Introduction

Hollow inorganic micro- and nanoparticles have attracted increasing interests because of their features of large interior spaces, low density, high specific surface area and well permeation properties with wide potentials in catalysis, chemical storage, ionic intercalation, surface functionalization, light weight fillers, battery electrodes, photonic crystals, and drug delivery carriers.[1–10] Much efforts have been exerted on developing synthetic strategies for fabricating inorganic hollow micro- and nanoparticles. Although the widely used hard template method was nearly a universal route for most hollow materials, this method usually suffers from the complicated processes, damaged structures during template removing and size limitation by the templates.[11–14] Recently, template-free methods have been successfully developed to fabricate hollow micro- and nanoparticles with tunable sizes, wall thickness and morphologies. These template-free routes generally involved Ostwald ripening, Kirkendall diffusion, or oriented attachment mechanisms.[15–20]

On the other hand, most of the documented results utilized the hydrothermal reactions to fabricate hollow nanostructures.[21-24] Hydrothermal reaction was indeed a facile strategy, but this route often suffered from the difficulty in scaling-up and process control. As was well-known, the addition of solutes usually elevated the boiling point of a solution. If the concentration was greatly increased, the boiling point would be intensively elevated. Practically, many so-called hydrothermal reactions were conducted below the boiling point. Some hydrothermal reactions are possibly replaced by a reflux method, which is process controllable and readily scaling-up.

We have hydrothermally prepared a series of perovskite hollow micro- and nanoparticles with tunable sizes.[21–24] The hollow $BaZrO_3$ microspheres exhibited excellent adsorptive capacities for reactive dyes and photoluminescence properties. [24] Herein, perovskite $BaZrO_3$ hollow microspheres were fabricated by a simple reflux method. The formation process was rationally discussed. $SrZrO_3$ and $SrHfO_3$ hollow nanoparticles were also prepared by this reflux method.

Experimental

Synthesis of $BaZrO_3$ hollow microspheres: All chemicals were analytical grade and used without purification. $BaZrO_3$ hollow nanospheres were prepared by refluxing mixtures of $ZrOCl_2{\cdot}8H_2O$ and $Ba(NO_3)_2$ in an aqueous KOH solution. Because of the intensively concentrated KOH solution was used, a three-neck Teflon vessel was utilized as the reactor. In a typical procedure, 17.92 g of KOH was added to a solution containing 0.538 g $ZrOCl_2{\cdot}8H_2O$ and 0.48 g $Ba(NO_3)_2$ in 20mL water under vigorous stirring. [*Cautions:* The dissolution of KOH in water caused a great heat release. If a large amount of KOH was directly dissolved in the reactant solution, the released dissolution heat would elevate the water temperature over 100 ℃ and led to the inhomogeneous formation of $BaZrO_3$ at ambient condition. In our synthetic procedure, KOH solution was pre-prepared and poured into the $ZrOCl_2{\cdot}8H_2O$, $Ba(NO_3)_2$ solutions after cooled to room temperature.] After the starting solution was stirred for 30

minutes at ambient temperature, the mixtures were refluxed in a 200 ℃ oil bath for 24 hours. The reactions produced white powders that were washed by distilled water, diluted acetic acid, absolute ethanol for several times and dried at 60 °C for 12 hrs. The yield was over 90% based on Zr. The output was facilely increased by proportionally augmenting the amount of the starting mixtures.

Physical characterization: Powder X-ray diffraction patterns were recorded on a Bruker D8 Advance X-ray diffractometer with Cu Kα radiation (λ = 1.5418 Å). The morphologies and microstructures of the as-synthesized hollow $BaZrO_3$ nanospheres were studied on Hitachi S-4800 field emission scanning electron microscope (SEM), Hitachi H-7650 transmission electron microscope (TEM, accelerating voltage 100 kV), and FEI Tecnai G2 F20 field emission transmission electron microscopy (HRTEM, accelerating voltage 200 kV). The energy dispersive X-ray (EDX) spectroscopy facility attached to the TEM was employed to analyze the chemical composition. The samples for TEM and HRTEM observations were prepared by dipping sonicated ethanol suspensions of $BaZrO_3$ powders onto the copper grids. The size distributions of the $BaZrO_3$ particles were evaluated by the TEM images of each sample to obtain statistically significant results.

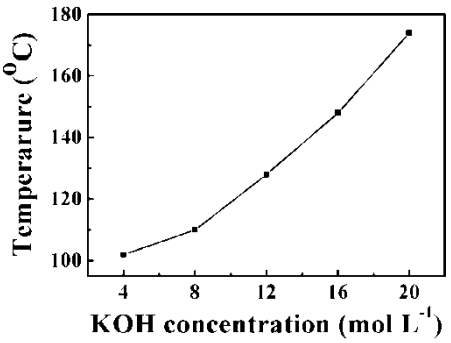

Figure 1 The concentration (within 20 mol Ł$^{-1}$) related boiling temperature of KOH solutions.

Results and Discussion

a. Morphological results and discussions

Dissolving solute in water was well-known to elevate the boiling temperature in most cases. When the KOH concentration was greatly increased, the boiling temperature was intensively increased (Figure 1). The boiling temperature of 20 mol Ł$^{-1}$ KOH solutions was up to 174 ℃, which was adequate to many synthetic reactions for inorganic materials. Although the boiling point of KOH solutions over 20 mol Ł$^{-1}$ was not measured, Figure 1 has indicated the relationship between the boiling temperature and the KOH concentration. Refluxing the starting mixtures of $ZrOCl_2{\cdot}8H_2O$ and $Ba(NO_3)_2$ in 20 mol Ł$^{-1}$ KOH solutions in a Teflon vessel produced white powders by setting the oil bath temperature at 200 ℃ for 24 hrs. The XRD patterns well matched to the cubic perovskite $BaZrO_3$ phase (JCPDS card 06-0399) (Figure 2a). TEM images revealed the hollow features of the spherical products with an average size of 92 nm and shell thickness of 9 nm (Figure 2b). Compared with the conventional statically hydrothermal synthesis,[24] the reflux reactions under stirring gave a narrow size distribution. HRTEM image of a single microsphere revealed that the lattice fringes were consecutive without obvious crystalline border, indicating the single crystal feature of a microsphere (Figure 2c). The spacing of the lattice fringes was 0.297 nm, which was associated with the (110) lattice plane of $BaZrO_3$. The well-shaped circle spots in the correlative SAED pattern further confirmed the single crystal nature (Figure 2d). The SEM image (Figure 1e) exhibited some holes on the microspheres, which further confirmed the hollow structures of the products. The EDS data (Figure 1f) disclosed the Ba:Zr ration of 0.96, which was close to the theoretical value. The presence of copper was originated from the copper grid. No other impurity element was detected.

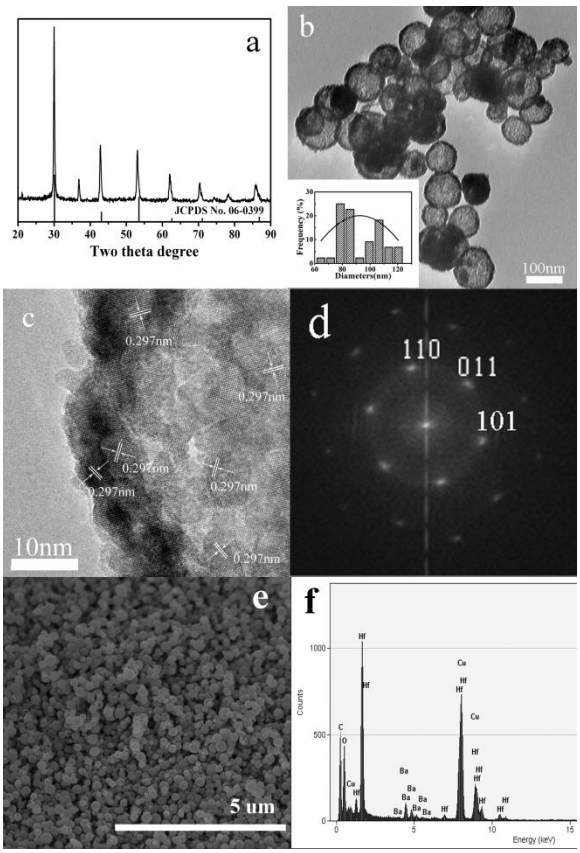

Figure 2 The XRD patterns (a), TEM (b) and HRTEM (c) images, SAED pattern (d), SEM image (e) and EDAX spectra of $BaZrO_3$ hollow microparticles prepared in 20 mol·L^{-1} KOH solutions at 200 °C for 24 hrs. Inset (b) is the size distribution histogram.

b. The effect of KOH concentration on the particle sizes

Changing the synthetic parameters greatly affected the formation of $BaZrO_3$ hollow microspheres. Investigations disclosed that the base concentration played a key role on the formation of $BaZrO_3$ hollow microspheres. The reactions in 8 mol·L^{-1} KOH solutions produced solid microspheres of 1−2 μm in sizes (Figure 3a). The products obtained in 12 mol·L^{-1} KOH solutions were still solid spheres with the particle sizes reduced to 1−1.3 μm (Figure 3b). Elevating the KOH concentration to 16 mol·L^{-1}, mixtures of core-shell microparticles and a few hollow particles formed with sizes in 200−400 nm (Figure 3c). Although a few particles did not fully hollowed, a strong contrast between the dark edges and the pale center of most particles indicated the

formation of hollow microspheres in 20 mol·L^{-1} KOH solutions (Figure 3d).

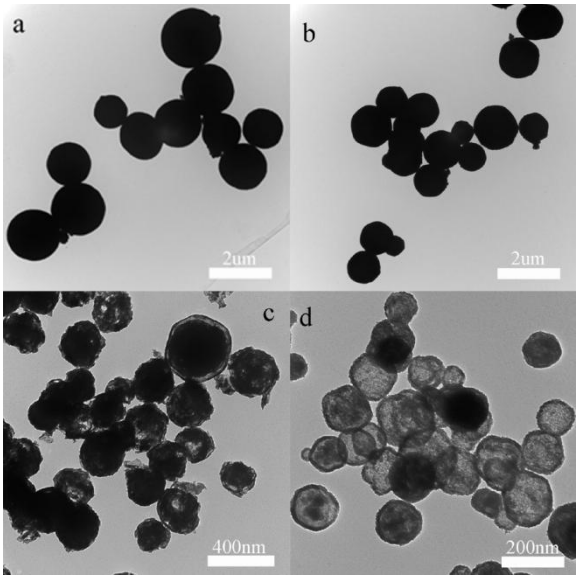

Figure 3 TEM images of the products synthesized in KOH solutions with various concentration at 200 °C for 24 hours, (a) 8 mol Ł$^{-1}$, (b) 12 mol Ł$^{-1}$, (c) 16 mol Ł$^{-1}$, (d) 20 mol Ł$^{-1}$.

c. The effect of temperature on the size and nucleation of microparticles

The oil bath temperature was another important factor (Figure 4). Heating the starting mixtures in 20 mol·L^{-1} KOH solutions in a 120 ℃ oil bath produced mixtures of solid and core-shell microspheres. Setting the bath temperature at 160 ℃ directed to the increase of the amount of core-shell microspheres. The reactions in a 180 ℃ oil bath produce more hollowed microspheres. High quality hollow nanospheres formed in a 200 ℃ oil bath.

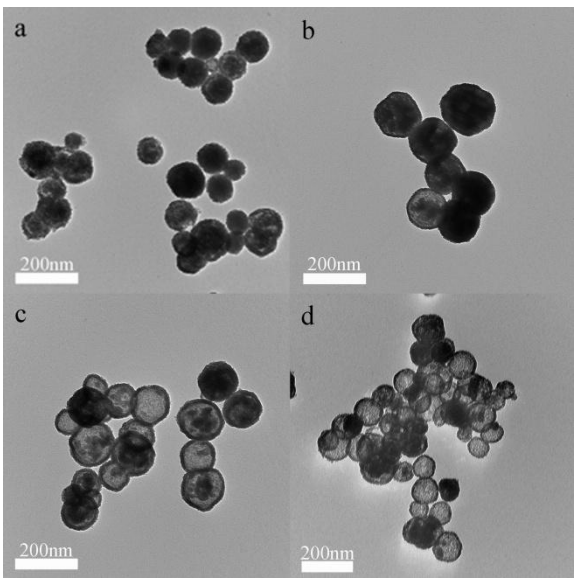

Figure 4 TEM images of the products synthesized at different oil bath temperature in 20 mol Ł$^{-1}$ KOH solutions for 24 hours, (a) 120 °C; (b) 160 °C; (c) 180 °C; (d) 200 °C.

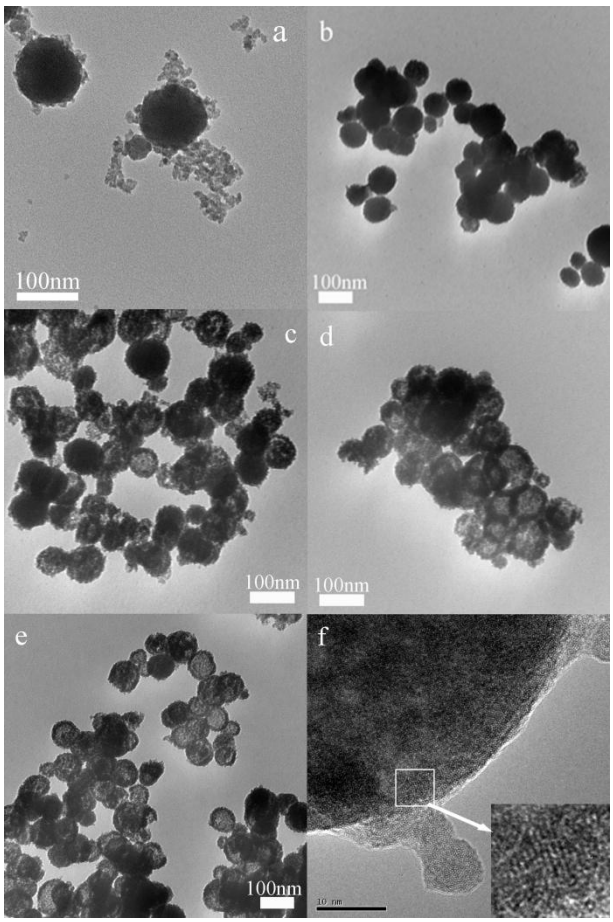

Figure 5 TEM images of the intermediates at various reaction durations in 20 mol Ł$^{-1}$ KOH solutions in a 200 °C oil bath, (a) before heating, (b) 1 hr, (c) 2 hrs, (d) 4 hrs, and (e) 8 hrs, and HRTEM image (f) of a single microsphere in (a). Inset (f) is a tiny crystallite in the microsphere.

d. The effect of reaction time on the size and nucleation of nanoparticles

To further study the formation mechanism, the intermediate products with different reaction durations were also studied in 20 mol·L^{-1} KOH solutions in a 200 ℃ oil bath. The spherical solid microparticles have formed before the heat treatment (Figure 5a). The rough surface and some attached tiny particulates implied that these spherical solid particles were assemblies of a large amount of tiny particulates. The presence of some ordered lattice fringes with sizes in 2 nm in HRTEM image of a single particle implied that some crystalline particulates have formed on the surface before heat treatment (Figure 5f). The distance of the lattice stripes agreed to that of cubic $BaZrO_3$. However, both the SAED and XRD patterns implied the amorphous nature of these aggregated particles. Based on the cell parameters of $BaZrO_3$, each of these tiny particulates only contained several cell units, which was hard to give an observable response to the X-ray or electron radiations. The microparticles were still solid microspheres with rough surfaces when the high temperature reactions were within one hour (Figure 5b). The suspended and attached particulates disappeared at this stage. The occurrence of a few voids in some particles implied the initiation of the hollowing process. Mixtures of solid, core-shell and hollow

microparticles formed within 2 hrs (Figure 5c). Extending the reaction time to 4 hrs, the core disappeared gradually with more hollow microparticles appeared (Figure 5d). Prolonging the time to 8 hrs, most microspheres transformed into hollow microparticles (Figure 5e). Further protracting the time to 24 hrs, the hollowing process completed to generate hollow microspheres. While the particle size was independent to the reaction time and kept constant, the crystallinity was positively related to the reaction duration that was revealed by the XRD patterns (Figure 6). The products were amorphous within 1 hour. The gradually intensified and narrowed XRD peaks also implied a size coarsing process.

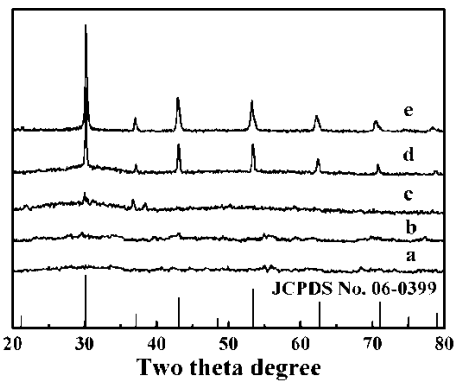

Figure 6 XRD patterns of $BaZrO_3$ hollow microspheres at various reaction durations in 20 mol L^{-1} KOH solutions in a 200 ℃ oil bath, (a) before heating, b) 1hr, c) 4 hrs, d) 8hrs, e) 24 hrs.

e. Discussions on the formation mechanism

Based on the synthetic parameters related results, the formation of $BaZrO_3$ hollow microspheres involved the Ostwald ripening process that was similar to the hydrothermal reactions. Ostwald ripening has been widely used to hydrothermally fabricate hollow micro- and nanoparticles of many binary compounds and some complex oxides.[4, 25, 26] The formation of $BaZrO_3$ hollow microspheres was assumed as follows. Zirconium cations readily hydrolyzed in base solutions to form soluble $Zr(OH)_5^-$ anions.[27] As well, barium cations formed $Ba(OH)^+$ species in concentrated KOH solutions.[28] The reactions between $Zr(OH)_5^-$ and $Ba(OH)^+$ initiated the nucleation and growth of the primary particulates to generate a sol-like suspension. As the base concentration was heavily increased, the solubility of the reactants was augmented to elevate the supersaturation of the reactant solutions. The intensively concentrated base solutions promoted a favourable nucleation over grain growth to form tiny primary particulates. Once the primary particulates appeared, they tend to aggregate into large particles due to the attractive van der Waals forces unless an electrostatic barrier erects.[29] In other words, these particulates readily agglomerated into aggregated particles to minimize the high surface energy. The aggregated particle sizes were dependent on the KOH concentration due to the influences of electrolyte concentration on the aggregation degree of primary particulates. Coagulation of the particulates was controlled by the sum of attractive van der Waals force and the electrostatic repulsion that was created by charges adsorbed on the particles. The repulsion barrier was dependent on the diffusive layer of the electrical double layer. Increasing the KOH concentration compressed the diffusive layer to reduce the repulsive barrier with the attractive force unchanged. This made an increase in the attractive interparticle potential and promoted the coagulation and destabilizing the sol. As a result, precipitation occurred at a smaller particle size by elevating the KOH concentration. This phenomenon has occurred in fabricating amorphous silica spheres with tunable sizes.[29] Heat treatment was unnecessary for the aggregation process. Due to the mineralization of the concentrated KOH solution, a few tiny crystallites formed on the particle surface. After the primary aggregated particles formed, the initiative recrystallization occurred through heat treatment at the solid-liquid interface of the nanospheres due to its affinity to the KOH solutions. Some suspended particulates were consumed by the large particles at this stage. Afterward, the solid spheres were subject to inside-out ripening. Voids were then produced to form core-shell particles due to the growth of the outer shell and consumption of the inner particulates. When the inner particulates were completely consumed by the shell, the hollowing process completed and left the large inner spaces empty. As a result, the products experienced solid, core-shell and hollow morphologies at various reaction durations. Also, the products transformed from amorphous particles, polycrystalline aggregated microparticles to single crystalline microspheres. Both the TEM images and XRD patterns confirmed the formation process. Although Ostwald ripening was the driving force, both the base concentration and reaction temperature greatly affected the hollowing process due to their influences on the chemical potentials and the diffusion rate. Since the boiling temperature and the aggregated particle size were related to the KOH concentration, both the large particle sizes and the lower reaction temperature in dilute KOH solutions were unfavourable to the hollowing process.

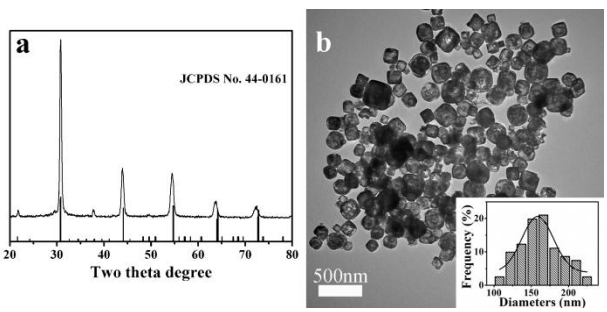

Figure 7 XRD pattern (a) and TEM image (b) of the cuboidal $SrZrO_3$ hollow microparticles that were fabricated in 34 mol L^{-1} KOH solutions in a 200 ℃ oil bath for 72 hours. Inset (b) is the size distribution histogram.

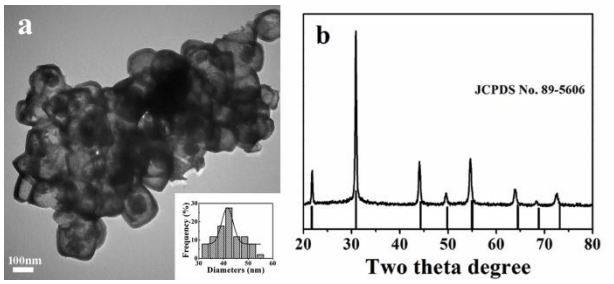

Figure 8 TEM image (a) and XRD pattern (b) of $SrHfO_3$ hollow microparticles that were fabricated in 32 mol L^{-1} KOH solutions in a 200 ℃ oil bath for 72 hours. Inset (a) is the size distribution histogram.

To extend the simple reflux method to hollow micro- and nanomaterials of other complex oxides, the syntheses of $SrZrO_3$ and $SrHfO_3$ hollow particles were also conducted. Unlike the formation of $BaZrO_3$ hollow microspheres, the formation of $SrZrO_3$ hollow micromaterials favoured more concentrated KOH solutions. This result was close to that of the hydrothermal routes.[21] Refluxing the starting mixtures in 34 mol Ł$^{-1}$ KOH solutions produced cuboidal $SrZrO_3$ hollow particles in submicrometer size (Figure 7b). The XRD patterns (Figure 7a) of the as-prepared sample indicated the monophasic feature with the diffraction peaks corresponding to the orthorhombic perovskite structure in the *Pnma* space group, which was in good agreement with the documented data (JCPDS No. 44-0161). TEM images revealed that the products were hollow particles with an average size of 158 nm. Aggregated cuboidal $SrHfO_3$ hollow microparticles with sizes of 200—300 nm were also produced in 32 mol Ł$^{-1}$ KOH solutions (Figure 8). The XRD patterns confirmed that the product was pure perovskite $SrHfO_3$ (orthorhombic space group *Pnma*) without any impurities.

Conclusions

In a summary, highly concentrated KOH solution was found to give a high boiling temperature. A simple reflux method was then developed to prepare hollow microparticles of complex oxide. Perovskite $BaZrO_3$ hollow microspheres have been synthesized by this method. Although high reaction temperature promoted the hollowing process it had no effect on the particle size. The concentration of KOH played the key role on the formation of hollow entities. The greatly elevated KOH concentration not only initiated a grain nucleation of $BaZrO_3$ to reduce the size of the aggregated particles but also afforded a high reaction temperature to promote the hollowing process. The formation of $BaZrO_3$ hollow microspheres was driven by Ostwald ripening. $SrZrO_3$ and $SrHfO_3$ hollow microparticles were also fabricated by using this method. This result contributed a feasible, scaling-up and process controllable strategy for fabricating metal oxide hollow micro- and nanoparticles.

Acknowledgments

The authors are grateful to the financial support by NSF of China (No. 21271138, 21371070, 21071060), NSF of Tianjin (No. 10JCZDJC21500) and the State Key Laboratory of Inorganic Synthesis and Preparative Chemistry of Jilin University (No. 2012-20)..

Notes and references

[a] *The State Key Laborotary of Inorganic Synthesis and Preparative Chemicstry, Jilin University, Changchun 130023, China. Fax: 86 431 85168516; Tel:86 431 85168624; E-mail: zouyc@jlu.edu.cn*
[b] *Institute of Nanostructured Materials & Tianjin Key Laboratory of Fiber Modification and Functional Fiber, School of Materials Science and Engineering, Tianjin Polytechnic University, Tianjin 300160, China. Fax: 86 22 24528055; Tel: 86 22 24528165; E-mail:zhaoyn@263.net*

1 Rapoport, L.; Bilik, Y.; Feldman, Y.; Homyonfer, M.; Cohen, S. R.; Tenne, R. *Nature* **1997**, *387*, 791.
2 Yin, Y. D.; Rioux, R. M.; Erdonmez, C. K.; Hughes, S.; Somorjai G. A.; Alivisatos, A. P. *Science* **2004**, *304*, 711.
3 Zeng, H. C. *J. Mater. Chem.* **2006**, *16*, 649.
4 Lou, X. W.; Archer L. A.; Yang, Z. C. *Adv. Mater*. **2008**, *20*, 1.
5 Zhang, Q.; Wang, W. S.; Goebl, J. Yin, Y. D. *Nano Today* **2009**, *4*, 494.
6 Peng, Q.; Dong, Y. J.; Li, Y. D. *Angew. Chem. Int. Ed.* **2003**, *42*, 3027.
7 Li, Y. Z.; Kunitake, T.; Fujikawa, S. *J. Phys. Chem. B* **2006**, *110*, 13000.
8 Shin, J.; Anisur, R. M.; Ko, M. K.; Im, G. H.; Lee J. H.; Lee, I. S. *Angew. Chem. Int. Ed.* **2009**, *48*, 321.
9 Zhao, W. R.; Chen, H. R.; Li, Y. S.; Li, L.; Lang M. D.; Shi, J. L. *Adv. Funct. Mater.* **2008**, *18*, 2780.
10 Sokolova, V. V.; Radtke, I.; Heumann, R.; Epple, M. *Biomaterials* **2006**, *27*, 3147.
11 Zhu, L. P.; Xiao, H. M.; Zhang, W. D.; Yang G.; Fu, S. Y. *Cryst. Growth Des.* **2008**, *8*, 957.
12 Wang, W. S.; Zhen, L.; Xu, C. Y.; Yang L.; Shao, W. Z. *J. Phys. Chem. C* **2008**, *112*, 19390.
13 Zhong, Z. Y.; Yin, Y. D.; Gates B.; Xia, Y. N. *Adv. Mater.* **2000**, *12*, 206.
14 Lou, X. W.; Yuan, C.; Rhoades, E.; Zhang Q.; Archer, L. A. *Adv. Funct. Mater.* **2006**, *16*, 1679.
15 Li J.; Zeng, H. C. *J. Am. Chem. Soc.* **2007**, *129*, 15839.
16 Yu, H. G.; Yu, J. G.; Liu S. W.; Mann, S. *Chem. Mater.* **2007**, *19*, 4327.
17 Yin, Y. D.; Erdonmez, C. K.; Cabot, A.; Hughes S.; Alivisatos, A. P. *Adv. Funct. Mater.* **2006**, *16*, 1389.
18 Liu B.; Zeng, H. C. *J. Am. Chem. Soc.* **2004**, *126*, 16744.
19 Chen, X. Y.; Qiao, M. H.; Xie, S. H.; Fan, K. N.; Zhou, W. Z.; He, H. Y. *J. Am. Chem. Soc.* **2007**, *129*, 13305.
20 Xu, H. L.; Wang W. Z.; Zhou, L. *Cryst. Growth Des.* **2008**, *8*, 3486.
21 Ye, T.; Dong, Z.; Zhao, Y.; Yu, J.; Wang, F.; Guo, S.; Zou, Y. *Langmuir* **2011**, *27*, 8878.
22 Ye, T.; Dong, Z.; Zhao, Y.; Yu, J.; Wang, F.; Guo, S.; Zou, Y. *Crytengcomm* **2011**, *13*, 3842.
23 Ye, T.; Dong, Z.; Zhao, Y.; Yu, J.; Wang, F.; Zhang, L.; Zou, Y. *Dalton Trans.* **2011**, 40, 2601.
24 Dong, Z.; Ye, T.; Zhao, Y.; Yu, J.; Wang, F.; Zhang, L.; Wang, X.; Guo, S. *J. Mater. Chem.* **2011**, *21*, 5978.
25 Xu, H. L.; Wang, W. Z.; Zhu, W.; L. Zhou, *Nanotechnology* **2006**, *17*, 3649.
26 Yang H. G.; Zeng, H. C. *J. Phys. Chem. B.* **2004**, *108*, 3492.
27 Baes, C. F.; Mesmer, R. E. in The Hydrolysis of Cations, Wiley-VCH, New York, USA, **1976**, Ch. 8.
28 Baes, C. F.; Mesmer, R. E. in The Hydrolysis of Cations, Wiley-VCH, New York, USA, **1976**, Ch. 5.
29 Brinker, C. J.; Scherer, G. W. in Sol-Gel Science: The Physics and Chemistry of Sol-Gel Processing, Academic Press, San Diego, USA, **1990**, Ch. 4.